View metadata, citation and similar papers at core.ac.uk
brought to you by CORE
provided by Elsevier - Publisher Connector

Available online at www.sciencedirect.com
SciVerse ScienceDirect
Energy Procedia 27 (2012) 503 – 509
Energy Procedia

SiliconPV: April 03-05, 2012, Leuven, Belgium

# Nickel silicide formation using excimer laser annealing

L. Tous[a,b,*], J-F Lerat[c], T. Emeraud[c], R. Negru[d], K. Huet[d], A. Uruena[b], M. Aleman[b], R. Russell[b], J. John[b], J. Poortmans[a,b], and R. Mertens[a,b]

[a] *Katholieke Universiteit Leuven (KUL), Oude Markt 13 Bus 5005, 3000 Leuven, Belgium*
[b] *Interuniversity Micro-electronic Center (imec), Kapeldreef 75, 3001 Leuven, Belgium*
[c] *EXCICO Group NV, Kempische Steenweg 305/2, B-3500 Hasselt Belgium*
[d] *EXCICO France SAS, 13-21 Quai des Grésillons, F-92230 Gennevilliers, France*

**Abstract**

In this work, we report on a self-aligned nickel silicide formation technique based on excimer laser annealing (ELA). We evaluate this process for the front contact formation of industrial PERC type solar cells on random pyramid textured Si surfaces where damage to surface texture, emitter passivation, or to the shallow junction should be avoided or minimized. PERC type solar cells obtained by $POCl_3$ diffusion were processed on large area (12.5x12.5 $cm^2$) CZ-Si. Self-aligned litho-free Ni/Cu contacts defined by ps-laser ablation of the $SiO_2/SiN_x$ anti-reflective coating (ARC) and subsequent ELA of the Ni layer were compared to conventional Ag screen printed contacts.
The novel ELA process results in an absolute gain in Jsc of 0.8 $mA/cm^2$ as well as a drop of 0.3 $\Omega.cm^2$ in series resistance (Rs) compared to SP Ag contacts due to reduced shading and resistance losses. This leads to 0.5% absolute increase in efficiency from 19.3% to 19.7% since other characteristics (Voc, pFF) could be maintained to the same level. In this work, the best performing cell with the ELA process reached an outstanding 20.0% energy conversion efficiency with Jsc=39.3 $mA/cm^2$, Voc=649.8mV, and FF=78.3%.

© 2012 Published by Elsevier Ltd. Selection and peer-review under responsibility of the scientific committee of the SiliconPV 2012 conference. Open access under CC BY-NC-ND license.

*Keywords:* Metallization; nickel; nickel silicides; laser annealing; solar cells

## 1. Introduction

Driven by the relatively high cost of silver (Ag), interest has grown in the Photovoltaic (PV) industry to substitute Ag by copper (Cu) contacts in a ‘seed and plate’ approach [1]. In this approach, self-aligned nickel (Ni) silicide contacts can be formed and subsequently covered with electroplated Cu to achieve the desired line conductivity.

* Corresponding author. Tel.: +32-162-875-22; fax: +32-162-875-22
*E-mail address*: loic.tous@imec.be

1876-6102 © 2012 Published by Elsevier Ltd. Selection and peer-review under responsibility of the scientific committee of the SiliconPV 2012 conference. Open access under CC BY-NC-ND license.
doi:10.1016/j.egypro.2012.07.101

Nickel silicides, formed by heating a stack of nickel and silicon (Si) at low temperature, have been well established in literature using conventional rapid thermal annealing (RTA) tools [2]. The formation of $Ni_2Si$, NiSi, $NiSi_2$ has been observed at different temperatures (250-300°C, 300-700°C and >700°C respectively). NiSi is the preferred phase for its excellent contact properties [2-3]. In PV, nickel silicide formation has been demonstrated using inline furnaces [4] or using dedicated RTA tools [5-6].

One significant challenge of nickel silicide formation is reducing the risk for shunting of the solar cell p-n junction while achieving excellent contact properties. In order to minimize the risk of junction shunting, results of self-aligned Ni/Cu contacts have been reported using deep p-n junctions formed by laser doping [7-8] or by two-step diffusions [5-6] adding complexity and costs to the process.

In this paper, we report on a novel nickel silicide formation process based on excimer laser annealing (ELA) which overcomes many of the limitations of conventional RTA. The ELA process consists in an original step-and-repeat approach to irradiate large portions of the wafer without damaging the emitter passivation. We study the impact of the ELA laser fluence on nickel silicide formation and on emitter dark saturation current densities. Finally, we demonstrate that the ELA process enables nickel silicide formation on shallow industrial emitters leading to high FF.

## 2. Experimental

In this work, nickel silicide formation was performed by irradiating a thin (40 nm) sputtered Ni layer with a, large area (10x10 $mm^2$), >150 ns pulse duration XeCl Excimer (308 nm) laser from EXCICO.

Large area (12.5x12.5 $cm^2$, area=149 $cm^2$) PERC type [9] solar cells were fabricated on standard commercial grade 1-3 Ω.cm, p-type, CZ-Si. The cells feature an industrial shallow type (< 400 nm) 85 Ω/sq emitter obtained by $POCl_3$ diffusion. Following diffusion, the junction isolation was performed in an inline one-side rear emitter removal tool [10]. Afterwards, the wafers were passivated on both sides with a thin thermal oxide grown at low temperature [11]. The SiNx ARC at the front and the $SiO_2/SiN_x$ passivation stack at the rear were deposited by PECVD. The local Al-BSF contacts at the rear were obtained by ns-laser ablation of the rear passivation stack, Al PVD deposition, and subsequent firing.

Standard screen printed Ag contacts were compared to self-aligned Ni/Cu contacts. In the latter case, the ARC was opened by ps-laser ablation (λ=355 nm). Subsequently, Ni was sputtered on top of the entire surface. Nickel silicidation was performed by ELA. The ELA was performed using a step-and-repeat approach (juxtaposition of 18x18 $mm^2$ laser spots) to irradiate the entire wafer area without damaging the passivation and optical properties of the ARC. After that, unreacted Ni was removed using a selective wet etch chemistry to form self-aligned nickel silicide contacts. Finally, the contacts were thickened using light induced plating of Ni (to achieve the desired line conductivity before Cu plating) and electroplating of Cu. Cu was capped using a thin Ag (<100 nm) deposited by immersion to prevent rapid Cu oxidation.

## 3. Results and discussions

### 3.1. Impact of ELA on random pyramid texture

The impact of the ELA on the front side texture, as shown in Fig.1 (a), was evaluated by measuring the reflectance at 700 nm as a function of ELA fluence on random pyramid textured CZ-Si.

At about 1 $J/cm^2$, the reflectance increases due to Si melting at the pyramid tips resulting in pyramid rounding as can be observed by scanning electron microscopy as shown in Fig.1 (b). Above 3 $J/cm^2$, the pyramids are entirely molten and the texture is destroyed. 1D COMSOL simulations of the ELA process

on planar Si [12] revealed that the threshold for Si melting is at 1.6 J/cm$^2$. The experimental threshold of 1 J/cm$^2$ on textured Si can be explained by heat trapping in the pyramid tips resulting in Si melting at lower laser fluence.

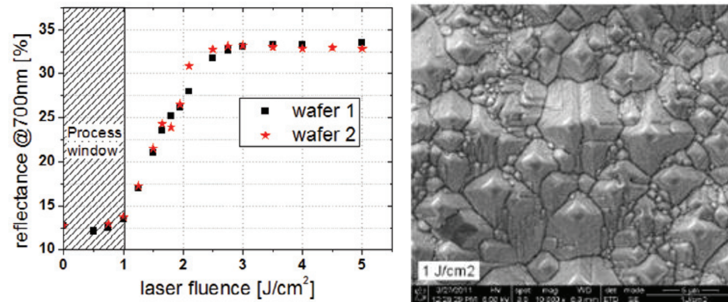


Fig. 1. (a) Reflectance measurements at 700 nm on random pyramid textured CZ-Si as function of laser fluence. (b) Scanning electron microscope (SEM) picture of a sample irradiated at 1 J/cm$^2$

### 3.2. Nickel silicide formation by ELA

Nickel silicide formation by ELA was evaluated by measuring sheet resistance ($R_{sheet}$) after ELA and selective removal of unreacted Ni. Wafers with a blanket 40 nm Ni layer received, in different locations, ELA shots with fluences ranging from 0.5 J/cm$^2$ to 2 J/cm$^2$. Measurements were performed using 4 point probe (4PP) in the centre of the 10x10 mm$^2$ shots on textured, chemically polished, and mirror polished CZ-Si substrates. The silicide thickness uniformity along the pyramid facets and tips was evaluated by taking transmission electron microscopy (TEM) pictures after removing unreacted Ni.

Fig. 2 shows the sheet resistance of nickel silicides formed as a function of laser fluence on textured, chemically polished, and mirror polished CZ-Si.

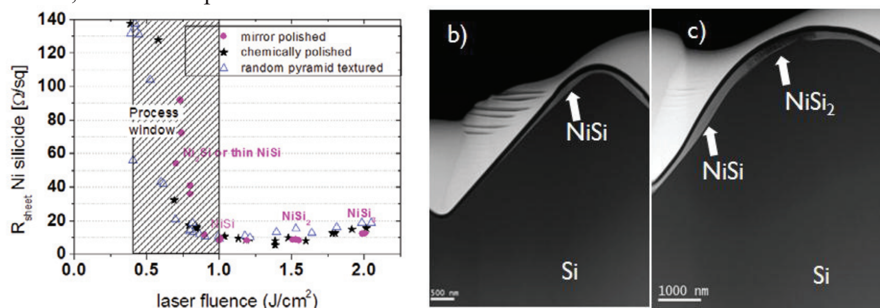


Fig. 2. (a) Sheet resistance ($R_{sheet}$) of the silicides formed as a function of laser fluence. Unreacted Ni was removed prior to measurement. The respective silicide phase compositions are indicated as measured by Rutherford Backscattering (RBS). (b) Transmission electron microscopy (TEM) picture of a sample irradiated at 0.55 J/cm$^2$. Energy dispersive X-ray spectroscopy (EDS) revealed the formation of NiSi. (c) TEM of a sample irradiated at 0.9 J/cm$^2$. EDS showed NiSi and $NiSi_2$ phase formation

Nickel silicides are formed at fluences as low at 0.5 J/cm$^2$. Possibly, this is due to the higher absorption of Ni in the UV region ($\lambda_{laser}$=308 nm). As a result melting of Si (T~1400°C) at the interface with Ni can be reached at much lower fluence (0.5 J/cm$^2$) than for bare Si (1.6 J/cm$^2$). This was confirmed by 1D COMSOL simulations and was shown to be strongly dependent on Ni thickness with thick layers (>1 µm) requiring more than 1.6 J/cm$^2$ to melt Si at the interface [12].

Rutherford backscattering measurements (RBS) were performed on mirror polished samples to determine phase composition (Fig. 2). RBS results indicate direct formation of NiSi at a fluence of around 1 J/cm$^2$ followed by the formation of the more resistive phases $NiSi_2$ and $NiSi_3$ above 1.5 J/cm$^2$. For lower fluences than 1 J/cm$^2$, the phase determination by RBS becomes difficult due to the too thin layers formed and hence Transmission electron microscopy (TEM) pictures were taken on pyramid textured samples to check the silicide phase and thickness. At 0.55 J/cm$^2$, a thin and continuous NiSi layer is directly formed. This is beneficial as NiSi is known for its better contact resistance properties [2]. The silicide thickness is larger at the pyramid tip possibly due to heat confinement leading to deeper Si melting. As expected from reflectance measurements, the pyramid tip is more rounded at 0.9 J/cm$^2$ due to Si melting. $NiSi_2$ formation occurred locally in the pyramid tip where the temperature reached was the highest. Additionally, the interface with Si is still smooth unlike with conventional RTA processing which sees an increase in interface roughness with increased sintering temperature [2, 6]. This is an important feature of ELA as high interface roughness has been reported to increase junction leakage in shallow junction devices [6].

These results indicate that nickel silicide formation by ELA follows liquid-state kinetics unlike conventional RTA which follows solid-state kinetics. In solid-state kinetics, direct formation of NiSi is not possible. $Ni_2Si$ is formed first at temperatures in the range 250-300°C, then converted to NiSi at 300-700°C, and finally to $NiSi_2$ for temperatures >700°C. As a result, a balance needs to be found between forming the low contact resistance phase NiSi and minimizing junction shunting which occurs faster at elevated temperatures due to high Si consumption and fast Ni diffusion [6]. On the contrary, ELA enables to form directly the low resistive NiSi phase while minimizing Si consumption as shown in Fig 3.

### 3.3. *Impact of ELA on emitter passivation*

The impact of ELA on the emitter was evaluated by measuring for different ELA fluences the emitter dark saturation current density $J_{0e}$ using the method described in [13]. Large area, p-type, 1-3 Ω.cm, CZ-Si wafers were random pyramid textured on both sides, then diffused (55 Ω/sq emitter) in a $POCl_3$ furnace, cleaned, and finally passivated on both sides by PECVD $SiN_x$. The wafers were fired in a fast firing oven and divided in 4 zones, as shown in Fig. 3, subjected to different ELA fluences. $J_{0e}$ and effective lifetime $\tau_{eff}$ were estimated using quasi-steady-state photo-conductance-calibrated photoluminescence (QSSPC-PL, BTI imaging). $J_{0e}$ and $\tau_{eff}$ were performed as well on high resistivity (Rho > 200 Ohm.cm) n-type polished FZ-Si wafers.

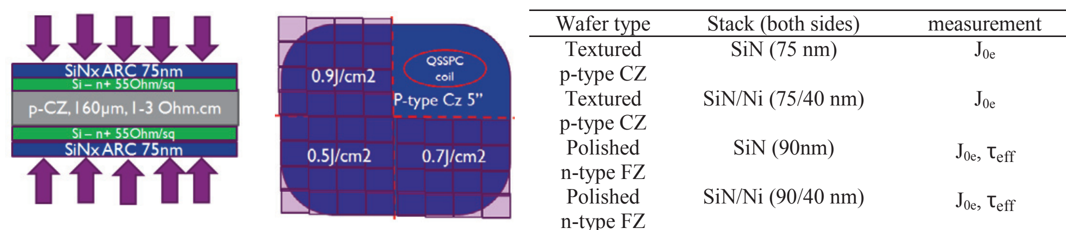


| Wafer type | Stack (both sides) | measurement |
|---|---|---|
| Textured p-type CZ | SiN (75 nm) | $J_{0e}$ |
| Textured p-type CZ | SiN/Ni (75/40 nm) | $J_{0e}$ |
| Polished n-type FZ | SiN (90nm) | $J_{0e}$, $\tau_{eff}$ |
| Polished n-type FZ | SiN/Ni (90/40 nm) | $J_{0e}$, $\tau_{eff}$ |

Fig. 3. Schematic of (a) the cross-section and (b) the ELA fluence used for the $J_{oe}$ samples (c) Summary table of $J_{oe}$ and $\tau_{eff}$ tests

In Fig. 4(a) it can be seen that $\tau_{eff}$~250 µs, comparable to the reference (REF) that did not receive ELA, can be achieved with 0.5 J/cm$^2$ when irradiating a Si/$SiN_x$ stack. This corresponds to the process sequence "A" where a thin Ni layer (<1 µm) would be selectively deposited (e.g. electroless Ni or Light Induced Plating (LIP)) in the $SiN_x$ openings and ELA would directly irradiate the un-metalized $SiN_x$

region. As a result, the process window would be rather narrow with 0.5 J/cm$^2$ required for silicide formation and 0.7 J/cm$^2$ already causing passivation damage. However, it should be noted that 1D COMSOL simulations showed that this could be the result of the thick (90 nm) $SiN_x$ layer coupling the 308 nm laser light better inside Si than with thinner $SiN_x$ (75 nm). In the latter case, a higher fluence (~ 0.9 J/cm$^2$) is required before melting Si [12]. With further optimization, a large enough process window could be found for ELA to work with industry compatible Ni deposition techniques such as LIP Ni and results will be reported elsewhere.

$\tau_{eff}$~250 µs can be maintained for ELA fluence as high as 0.9 J/cm$^2$ when the $SiN_x$ is protected by 40 nm of PVD Ni as shown in Fig. 4 (b). This corresponds to the process sequence "B" where Ni is sputtered over the entire wafer area and self-aligned nickel silicides contacts are formed by ELA.

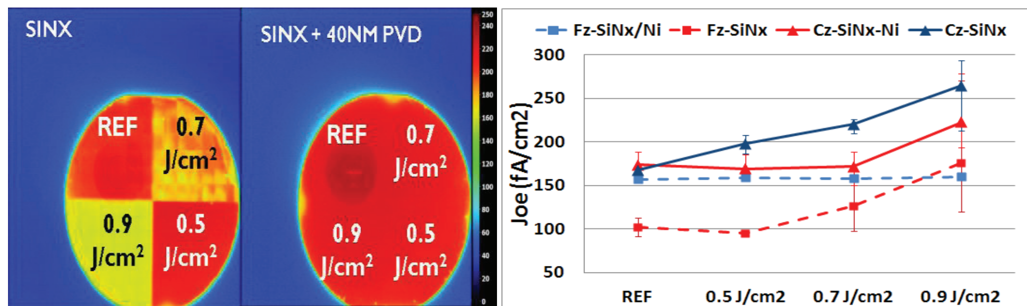


Fig. 4. Calibrated $\tau_{eff}$ at 1x10$^{16}$ cm$^{-3}$ as obtained from QSSPC-PL on n-type FZ wafers as function of ELA fluence on (a) Si/$SiN_x$ (90 nm) and (b) Si/$SiN_x$/Ni (90/40 nm). (c) $J_{0e}$ as obtained from QSSPC-PL on high resistivity n-type FZ wafers and p-type textured CZ wafers for different ELA fluences. In the case of a $SiN_x$/Ni stack, Ni was removed prior to measuring $\tau_{eff}$ or $J_{0e}$

$J_{0e}$ results, averaged over 3 wafers, for both p-type textured CZ-Si and n-type polished FZ-Si wafers, are summarized in Fig. 4 (c). Using a Si/$SiN_x$/Ni stack, low $J_{0e}$~170 fA/cm$^2$ can be maintained up to 0.7 J/cm$^2$ on textured CZ-Si and up to 0.9 J/cm$^2$ on polished FZ-Si. The reduced process window for textured samples is believed to be the result of Si melting occurring at lower fluence in the pyramid tips as shown previously. Finally, comparing the un-irradiated (REF) $J_{0e}$ results on FZ-Si, it is observed that the Si/$SiN_x$ stack ($J_{0e}$~100 fA/cm$^2$) yields significantly lower $J_{0e}$ values than the Si/$SiN_x$/Ni stack ($J_{0e}$~170 fA/cm$^2$). This is possibly the result of sputter-induced damage during the Ni PVD as already reported for Al PVD on $SiO_2$ films [14]. Though the achieved $J_{0e}$ values after ELA of the Si/$SiN_x$/Ni stack (process sequence "A" with PVD Ni) were lower than after ELA of the Si/$SiN_x$ stack (process sequence "B"), PVD Ni was chosen to demonstrate ELA at cell level since it offers better Ni thickness control and repeatability.

### *3.3. Solar cell results*

Table 2 shows the I-V characteristics of large area PERC solar cells featuring either screen printed (SP) Ag front contacts or litho-free Ni/Cu front contacts where silicide formation was performed by ELA.

Table 2. I-V characteristics of large area (12.5x12.5 $cm^2$) PERC type cells featuring an industrial shallow emitter (~85 Ω/sq)

| Device | $J_{sc}$ [$mA/cm^2$] | $V_{oc}$ [mV] | FF [%] | Eta [%] | Rs [$Ω.cm^2$] | pFF [%] |
|---|---|---|---|---|---|---|
| Average SP (6 cells) | 38.3 ±0.1 | 651.3 ±2.1 | 77.3 ±1 | 19.3 ±0.2 | 1.1 ±0.1 | 83.2 ±0.3 |
| best SP | 38.4 | 653.5 | 77.8 | 19.5 | 1.0 | 83.4 |
| Average ps-laser + ELA (5 cells) | 39.1 ±0.3 | 649.2 ±1.1 | 77.7 ±1 | 19.7 ±0.2 | 0.8 ±0.2 | 82.2 ±0.1 |
| Best ELA | 39.3 | 649.8 | 78.3 | 20.0 | 0.7 | 82.1 |
| Absolute difference with SP | 0.8 | -2.1 | 0.4 | 0.5 | -0.3 | -1.1 |

The ELA process enabled an absolute gain in $J_{sc}$ of 0.8 $mA/cm^2$ as well as a 0.3 $Ω.cm^2$ drop in series resistance (Rs) compared to SP Ag contacts. This is explained by reduced shading and resistance losses. These gains directly translate in a $0.5\%_{abs.}$ increase in efficiency from 19.3% to 19.7% since other characteristics ($V_{oc}$, pFF) were maintained to a similar level. The best cell with this ELA process reached an outstanding 20% energy conversion efficiency with $J_{sc}$=39.3 $mA/cm^2$, $V_{oc}$=649.8mV, and FF=78.3%.

The high pFF obtained with the ELA process indicates that junction shunting of the shallow 85 Ω/sq emitter could be minimized using optimized process conditions. However, the long-term integrity of the shallow junction to both Cu and Ni diffusion remains questionable. Therefore, in the next phase, accelerated thermal tests as proposed in Ref. [15] will be performed together with standard IEC 61215 (thermal cycling and 85ºC/85% relative humidity) testing.

## 4. Conclusions

In this work, we characterized nickel silicide formation by excimer laser annealing (ELA). Direct formation of the NiSi phase was shown at low laser fluence (0.5 $J/cm^2$) while minimizing Si consumption and interface roughness. In addition, passivation properties could be maintained up to 0.7 $J/cm^2$ on textured CZ-Si. This enabled nickel silicide formation by ELA using an original step-and-repeat approach to irradiate large portions of the wafer without damaging the emitter passivation. Finally, using this novel ELA process, we report energy conversion efficiency up to 20.0% on large area PERC type solar cells featuring and industrial shallow homogeneous emitter (~85 Ω/sq).

## Acknowledgements

The authors greatly acknowledge the support of S. Singh for PVD processing as well as J. Meersschaut for the RBS measurements and H. Bender for the TEM analysis.

## References

[1] Dubé C. E. and Gonsiorawski R.C., Improved contact metallization for high efficiency EFG polycrystalline silicon solar cells, *Proc. of the 21st IEEE PVSC*, Kissimmee, USA, 1990

[2] A. Lauwers et al., Ni based silicides for 45 nm CMOS and beyond, *MSE*, Vol. B 114–115, pp29–41, 2004

[3] Stavitski N., van Dal M. J. H., Lauwers A., Vrancken C., Kovalgin A. Y., and Wolters R. A. M., Systematic TLM Measurements of NiSi and PtSi Specific Contact Resistance to n- and p-Type Si in a Broad Doping Range, *IEEE EDL*, 29 (4), 2008

[4] Bay N., Burschik J., Cimiotti G., Fritz N., Kösterke N., Kray D., Lösel A., Lühn O., Sieber M., Träger A., Kühnlein H.H., Nussbaumer H., Adhesive one step Ni/Ag and Ni/Cu/Ag inline direct plating on laser processed selective emitter structures, *Proc. of the 25th EUPVSEC*, Valencia, Spain, 2011

[5] Tous L., Russell R., Das J., Labie R., Ngamo M., Horzel J., Philipsen H., Sniekers J., Vandermissen K., van den Brekel L., Janssens T., Aleman M., van Dorp D.H., Poortmans J., Mertens R., Large area copper plated silicon solar cell exceeding 19.5% efficiency, *Proc. of the 3rd metallization workshop*, Charleroi, Belgium, 2011

[6] Tous L., van Dorp D.H., Hernandez J-L, Allebe C., Ngamo M., Bender H., Meersschaut J., Alemán M., Russell R., Poortmans J., and Mertens R. Minimizing juction damage associated with nickel silicide formation for the front side metallization of silicon solar cells, *Proc. of the 26th EUPVSEC*, Hamburg, Germany, 2011

[7] B. Hallam B., Wenham S., Sugianto A., Mai L., Chong C., Edwards M., Jordan D., Fath P., Record large area p-type Cz production cell efficiency of 19.3% based on LDSE technology, *Proc. of the 36th IEEE PVSC*, Seattle, USA, 2011

[8] Kray D, Alemán M, Fell A, Hopman S, Mayer K, Mesec M, Müller R, Willeke GP, Glunz SW, Bitnar B, Neuhaus D-H, Lüdemann R, Schlenker T, Manz D, Bentzen A, Sauar E, Pauchard A, and Richerzhagen B. Laser-doped Silicon Solar Cells by Laser Chemical Processing (LCP) exceeding 20% Efficiency, *Proc. of the 33rd Photov. Spec. Conf*, San Diego, USA, 2008

[9] G. Agostinelli, *Proc. of the 21st EUPVSEC*, Dresden, Germany, 2006

[10] E. Cornagliotti et al., *this conference*

[11] V. Prajapati et al., *Proc. of the 38th PVSC*, Austin, USA, 2012

[12] J-F. Lerat, *Proc. of the 27th EUPVSEC*, Frankfurt, Germany, 2012

[13] Cuevas A. et al., Surface recombination velocity of highly doped n-type silicon, *JAP 80 (6)*, 1996

[14] Reed M.L., Plummer J.D., Chemistry of SiSiO2 interface trap annealing, *JAP, 63 (12)*, 1988

[15] Bartsch J et al. Quick determination of copper metallization long term impact on silicon solar cells, *J. ECS. 157 (10)*, 2010